

THE MICROSTRUCTURAL RECORD OF PREDATION: A NEW APPROACH FOR IDENTIFYING PREDATORY DRILL HOLES

JAMES D. SCHIFFBAUER,^{1*} YURENA YANES,² CARRIE L. TYLER,¹ MICHAŁ KOWALEWSKI,¹ and LINDSEY R. LEIGHTON³

¹Department of Geosciences, Virginia Polytechnic Institute and State University, 4044 Derring Hall, Blacksburg, Virginia 24061, USA;

²Savannah River Ecology Laboratory, University of Georgia, Drawer E, Aiken, South Carolina 29802, USA;

³Department of Earth and Atmospheric Sciences, University of Alberta, Edmonton, Alberta, T6G 2E3 Canada

e-mail: jdschiff@vt.edu

ABSTRACT

Drill holes in prey skeletons are the most common source of data for quantifying predator-prey interactions in the fossil record. To be useful, however, such drill holes need to be identified correctly. Field emission scanning electron microscopy (FE-SEM) and environmental scanning electron microscopy (ESEM) were applied to describe and quantify microstructural characteristics of drill holes. Various specimens, including modern limpets and mussels drilled by muricid snails in laboratory experiments, subfossil limpets collected from a tidal flat (San Juan Island, Washington state, USA), and various Miocene bivalves collected from multiple European sites, were examined for microstructural features. The microstructures observed are interpreted here as *Radulichnus*-like micro-rasping marks, or predatory microtraces, made by the radula of drilling gastropod predators. The mean adjacent spacing of these microtraces is notably denser than the spacing of muricid radular teeth determined by measurements taken from the literature. Because the radular marks typically overlie or crosscut each other, the denser spacing of predatory microtraces likely reflects superimposition of scratches from repeated passes of the radula. One incomplete drill hole showed a clear, chemically aided drilling dissolution signature around its outer margin, while a number of other specimens showed similar, but ambiguous, traces of dissolution. The range of organisms examined illustrates the utility of scanning electron microscopy (SEM) imaging for identifying micro-rasping marks associated with predatory drill holes in both modern and fossil specimens. These distinct microtraces offer promise for augmenting our ability to identify drill holes in the fossil record and to distinguish them from holes produced by non-predatory means.

INTRODUCTION

Drill holes bored by predators in prey shells provide direct data on predator-prey interactions and have been widely used by paleontologists to quantify predation patterns in the fossil record (e.g., Vermeij, 1987; Kowalewski et al., 1998, 2005; Leighton, 2001, 2003; Kelley and Hansen, 2006; Huntley and Kowalewski, 2007 and numerous references therein). Many qualitative and quantitative assumptions, however, are involved in applying drill holes to study the fossil record of predation (see Kowalewski, 2002; Walker, 2007 for detailed reviews), including the fundamental issue of correctly distinguishing traces produced by drilling predators from those produced by other biotic and abiotic agents (e.g., Kaplan and Baumiller, 2001; Wilson and Palmer, 2001). Specifically, two main

types of diagnostic errors can be anticipated: (1) traces other than predatory drill holes (i.e., substrate borings, non-predatory dissolution or bio-erosion, punctures, fixichnia, etc.) are misidentified as drillings of predatory origin (Lescinsky and Benninger, 1994); and (2) true drill holes are not identified as predatory in origin. Both of these errors may be particularly frequent when the examined fossils have been significantly degraded. In such cases, “false” drill holes may form by taphonomic processes and “true” drill holes may remain unidentified due to their poor preservation.

Efforts to mitigate identification errors have focused so far on two independent strategies: (1) the use of non-morphological criteria, such as evaluating holes for non-random (site-specific, size-selective, or taxon-restricted) distribution of traces (e.g., Sheehan and Lesperance, 1978; Kitchell et al., 1981; Kelley, 1988; Leighton, 2002; Hoffmeister et al., 2003) and (2) morphometric strategies focused on quantifying drill-hole shapes (e.g., Kowalewski, 1993; Urrutia and Navarro, 2001; Grey et al., 2005; Diel and Kelley, 2006). Here, we explore a third approach based on physical and chemical microstructural criteria: micron-scale predatory signatures (predatory microtraces) of drill holes that can be recognized and examined through high-magnification, high-resolution imaging under field emission and environmental scanning electron microscopy (FE-SEM and ESEM, respectively).

The microstructural approach builds directly on the pioneering work of Carriker (1969, 1978) and Carriker and Van Zandt (1972), who used SEM micrographs to study microstructural details of drill holes bored by modern snails in oysters and mussels. Substantial advances in nano-imaging technology, taphonomy, and paleoecology make this approach a particularly promising strategy for augmenting our ability to identify drill holes found in fossil prey correctly.

This study represents a first step towards establishing and using microstructural criteria to identify predatory drillings. We focus on comparing microstructural details of drillings in a range of taxa from laboratory feeding experiments and field collections of both subfossil and fossil shells. Specifically, we have evaluated micron-scale features of drill holes made by muricid gastropod predators in both limpets and mussels from laboratory settings at Friday Harbor Laboratories (FHL), San Juan Island (University of Washington). In addition, we have examined subfossil limpet specimens collected from a modern tidal-flat setting (San Juan Island, Washington state, USA) and various bivalve fossil samples collected from marine Miocene bioprovinces of Europe, including the Boreal province, Paratethys, and southeast North Atlantic (Kowalewski et al., 2002). This range of organisms illustrates the utility of SEM image analysis to identify radular microtraces of predatory drill holes. Moreover, the integration of observations from feeding experiments with analyses of subfossil and fossil material makes it possible to assess the detrimental effects of taphonomic processes on microtraces of predatory drill holes and evaluate the preservation potential of these microtraces in the fossil record. The initial data reported here suggest

* Corresponding author.

that microstructural criteria may indeed facilitate the identification of drill holes in the fossil record.

MATERIALS AND METHODS

Sample Collection and Laboratory-Feeding Experiment Protocol

Laboratory-Observed Limpets.—All studied lottiid prey and muricid predators were collected from rocky intertidal habitats of False Bay, located on the southwest coast of San Juan Island. Collection for the feeding experiments focused on two limpet species, coarsely ribbed *Lottia digitalis* (Rathke) and smooth-shelled *Tectura scutum* (Rathke), both of which are known to be prey species. One species of drilling predator, the muricid gastropod *Nucella ostrina* (Gould) (common name, northern striped dogwinkle) was also collected. These three species are highly abundant, readily accessible for collecting, and overlap spatially in their distribution in the study area.

To examine examples of drilling known to be made by the muricid *Nucella*, 100 specimens of *N. ostrina* and 120 limpets (60 of *L. digitalis* and 60 of *T. scutum*) were housed in an open-circulation sea table at FHL. The prey had freedom of movement and were readily accessible to each predator individual. Salinity and temperature, which were monitored daily in the open-circulation system, were relatively stable during the month-long laboratory observation period ($30.5‰ \pm 0.8‰$ and $13.5^\circ \pm 0.9^\circ\text{C}$, respectively). Only two drilled limpets (*L. digitalis* and *T. scutum*) were obtained in the laboratory, as the muricid gastropods in the laboratory setting were not as active as anticipated.

The two drilled limpets were collected after being abandoned by their predator (no predation attempts were manually interrupted), and any remaining limpet soft tissue was removed from the shell. The predator responsible for the kill was photographed and its shell maximum length and width were measured with digital calipers to the nearest 0.1 mm. In order to protect local dogwinkle and limpet populations, all individuals still alive at the end of the experiment were returned to the original sampling locale.

Laboratory-Observed Mussels.—The mussel samples examined came from a previously published experimental study (Kowalewski, 2004). Mytilid prey and their muricid predators were originally collected from Argyle Creek, a narrow channel connecting Argyle Lagoon and North Bay, San Juan Island. Kowalewski (2004) used the mussel *Mytilus trossulus* (Gould) and the gastropod predator *Nucella lamellosa* (Gmelin) (common name, frilled dogwinkle) in laboratory-feeding experiments. He also noted that empty *Mytilus* shells with predatory drill holes were abundant at the sample site, and that snails were commonly observed actively feeding on mussels (Kowalewski, 2004). These two organisms not only co-occur naturally, but also represent an important predator-prey interaction within the creek habitat (Kowalewski, 2004).

The current study examined six mussels drilled by two predator individuals; the six were selected from the Virginia Tech repository of 76 drilled mussels from the feeding experiment reported by Kowalewski (2004). Using the same FHL facilities as employed for the limpet feeding experiment, Kowalewski (2004) placed ~ 100 specimens of *N. lamellosa* and several hundred *M. trossulus* specimens into two open-circulation sea tables. The gastropod predators were permitted to hunt freely until observed attacking prey. During the attack, the snail and mussel were caged in a meshed container and allowed to finish their attack unobstructed and uncontested. Abandoned prey shells were collected, predators were recorded, and all individuals, predator and prey, were measured. All individuals alive at the end of the experiment were returned to the original sampling locale, with the exception of two predatory dogwinkles that drilled the shells examined for this study; these were stored in ethyl alcohol.

Subfossil Limpets.—Three bulk samples of subfossil shell remains (including complete and fragmented shells) were randomly collected from a single surficial shell assemblage from the same intertidal region of False Bay as the live specimens. Each bulk sample, which consisted of ~ 1 kg

of shell remains of multiple organisms, was first cleaned, sorted for limpet shells, and then examined for the presence of possible drill holes. Drill holes of probable or possible predatory origin were identified by measuring the circular regularity of the outline under reflected light microscopy. In total, ten limpets with putative drill holes were selected for SEM analysis. Drilled *T. scutum* individuals were exceedingly rare in the subfossil bulk samples, and consequently only *L. digitalis* specimens are included in the FE-SEM examination of subfossil material.

Miocene Bivalves.—The examined Miocene samples came from a previously published study (Kowalewski et al., 2002; see also Hoffmeister and Kowalewski, 2001), in which a total of 24 bulk samples were collected from 13 Miocene localities spanning central and western Europe. Specimens were selected from the Virginia Tech repository on the basis of range of sampling locales, in an effort to examine material from each of the sampled bioprovinces and ages. Drill holes of probable predatory origin were first examined under reflected light, and a total of twelve specimens were chosen for SEM analysis. These included eight specimens of *Astarte radiata* (Nyst and Westendorp) from Burdigalian deposits (early Miocene, sample age of 16.5 Ma) of the Boreal province, from the Winterswijk-Miste area (Netherlands); one *Clausinella basteroti* (Deshayes) from Langhian deposits (middle Miocene, sample age of 15.5 Ma) of the Paratethys, Szabó Quarry (Várpalota Basin, Hungary), and three specimens (*Callista* sp. [Lamarck], *Anadara diluvii* [Lamarck], and *Callucina dujardini* [Dall]) from Serravallian deposits (middle Miocene, sample age of ~ 14 Ma) of the southeastern North Atlantic province, from Ferrière Larçon (Loire River, France) (Kowalewski et al., 2002).

The sampled material was deposited in the Department of Geosciences at Virginia Polytechnic Institute and State University (Virginia Tech). Specimen identification numbers are provided in Table 1 and throughout the text where applicable.

Scanning Electron Microscopy

Randomly located drill holes bored by muricid gastropods in limpets and mussels in the laboratory setting and putative, randomly located drill holes identified in field-collected subfossil limpets and fossil bivalves were analyzed using field-emission scanning electron microscopy (LEO 1550 FE-SEM) or environmental scanning electron microscopy (FEI Quanta 600 FEG). All limpet specimens were sputter-coated with a gold-palladium mixture (20 nm thickness in a Cressington 208HR high resolution sputter coater) and analyzed via FE-SEM. The laboratory-drilled mussels and Miocene bivalves were imaged via ESEM in low-vacuum mode without gold-palladium coating, in order to avoid possibly obscuring submicron-scale features of interest (e.g., shell crystalline microarchitectures). The brightness (or shadowing) effects observed for various features of the drill holes, when utilizing secondary electron detection in either FE-SEM or ESEM, indicate areas receiving more (or less) electron beam interaction, thus demonstrating simulated three-dimensional surface relief that represents topographic sculpture of the external drill-hole surfaces. Each electron micrograph was examined with ImageJ[®] or Adobe Photoshop[®] CS2 software, both of which permitted the collection of precise numerical measurements of the drill holes, including (1) spacing between the microrasping marks produced by the teeth of the radula; (2) distance between microrasping marks and the inner-hole margin; and (3) overall diameter of the drill-hole opening. These numerical measures were taken in order to quantitatively describe the preserved microstructures in and around the observed drill holes. The ESEM micrographs of uncoated mussels presented an opportunity to collect data on the crystalline microarchitecture of the shells possibly related to the radular rasping microtraces. These features were also imaged and analyzed via Photoshop[®] CS2 as were two published scanning electron micrographs of the radula of the dogwhelk, *Nucella lapillus* (Linnaeus) (Rolán et al., 2004) for comparative purposes. This specific publication was chosen because the illustrated radulae were from drilling predators congeneric to those used in the two laboratory feeding experiments (*N. ostrina* in the

TABLE 1—Descriptive statistics for the quantified predatory microtraces, shell-growth microfabrics, and radular cusp measurements from Rolán et al. (2004). Symbols: Specimen ID = Virginia Tech repository number; n = number of measured rasp marks; SD = standard deviation; Max = maximum size measured; Min = minimum size measured.

Specimen ID#	Species	Sample origin	n	Mean (μm)	SD (μm)	Max (μm)	Min (μm)
VT-P-001	<i>Lottia digitalis</i>	Laboratory-observed limpets	42	11.18	3.16	20.04	6.88
VT-P-002	<i>Tectura scutum</i>	Laboratory-observed limpets	88	5.38	1.45	10.28	2.94
Pooled laboratory-observed limpets			130	7.25	3.47	20.04	2.94
VT-MT-17 (predator NL-16)	<i>Mytilus trossulus</i>	Laboratory-observed mussels	13	8.67	3.37	17.67	4.17
VT-MT-52 (predator NL-16)	<i>M. trossulus</i>	Laboratory-observed mussels	132	8.61	3.58	21.67	1.84
VT-MT-53 (predator NL-16)	<i>M. trossulus</i>	Laboratory-observed mussels	26	8.44	2.21	13.25	5.21
VT-MT-72 (predator NL-16)	<i>M. trossulus</i>	Laboratory-observed mussels	18	8.14	1.68	11.76	5.56
VT-MT-48 (predator NL-34)	<i>M. trossulus</i>	Laboratory-observed mussels	42	6.47	2.02	10.86	3.49
VT-MT-68 (predator NL-34)	<i>M. trossulus</i>	Laboratory-observed mussels	47	8.69	2.29	16.13	5.07
Pooled laboratory-observed mussels			278	8.26	3.04	21.67	1.84
VT-2-3 C-3, subfossil limpet	<i>L. digitalis</i>	Subfossil limpet assemblage	16	8.24	1.81	10.69	4.35
VT-1-4 B-3, subfossil limpet	<i>L. digitalis</i>	Subfossil limpet assemblage	12	4.72	0.89	6.09	3.58
VT-2-3 B-10, subfossil limpet	<i>L. digitalis</i>	Subfossil limpet assemblage	10	6.37	1.49	9.85	4.51
VT-1-6 B-1, subfossil limpet	<i>L. digitalis</i>	Subfossil limpet assemblage	15	13.03	2.47	17.31	9.68
Pooled subfossil limpets			53	8.44	3.64	17.31	3.58
VT-B5-3-1	<i>Astarte radiata</i>	Winterswijk-Miste, Burdigalian Stage	50	6.92	1.71	10.68	3.86
VT-B5-3-4	<i>A. radiata</i>	Winterswijk-Miste, Burdigalian Stage	25	10.47	1.66	13.58	7.25
VT-S14-11	<i>Clausinella basteroti</i>	Szabó Quarry, Langhian Stage	88	5.13	1.34	8.83	2.51
Pooled Miocene bivalves			163	6.50	2.40	13.58	2.51
Total pooled predatory microstructures			624	7.60	3.13	21.67	1.84
Additional structures of note							
Pooled crystalline shell microfabrics			152	1.37	0.39	2.57	0.53
Radular cusp width			45	15.26	2.18	21.36	11.53
Multiple-pass versus single-pass rasp marks							
Multiple-pass microstructures			149	5.75	1.79	11.21	1.84
Single-pass microstructures			108	10.31	3.25	21.67	4.18

limpet-feeding experiment and *N. lamellosa* in the mussel-feeding experiment). The measurements assessed from these micrographs consisted of basal widths of the cusps from each rachidian tooth. PAST software (Hammer et al., 2001) was used for univariate statistical analyses.

RESULTS

Overview of Microtrace Morphology

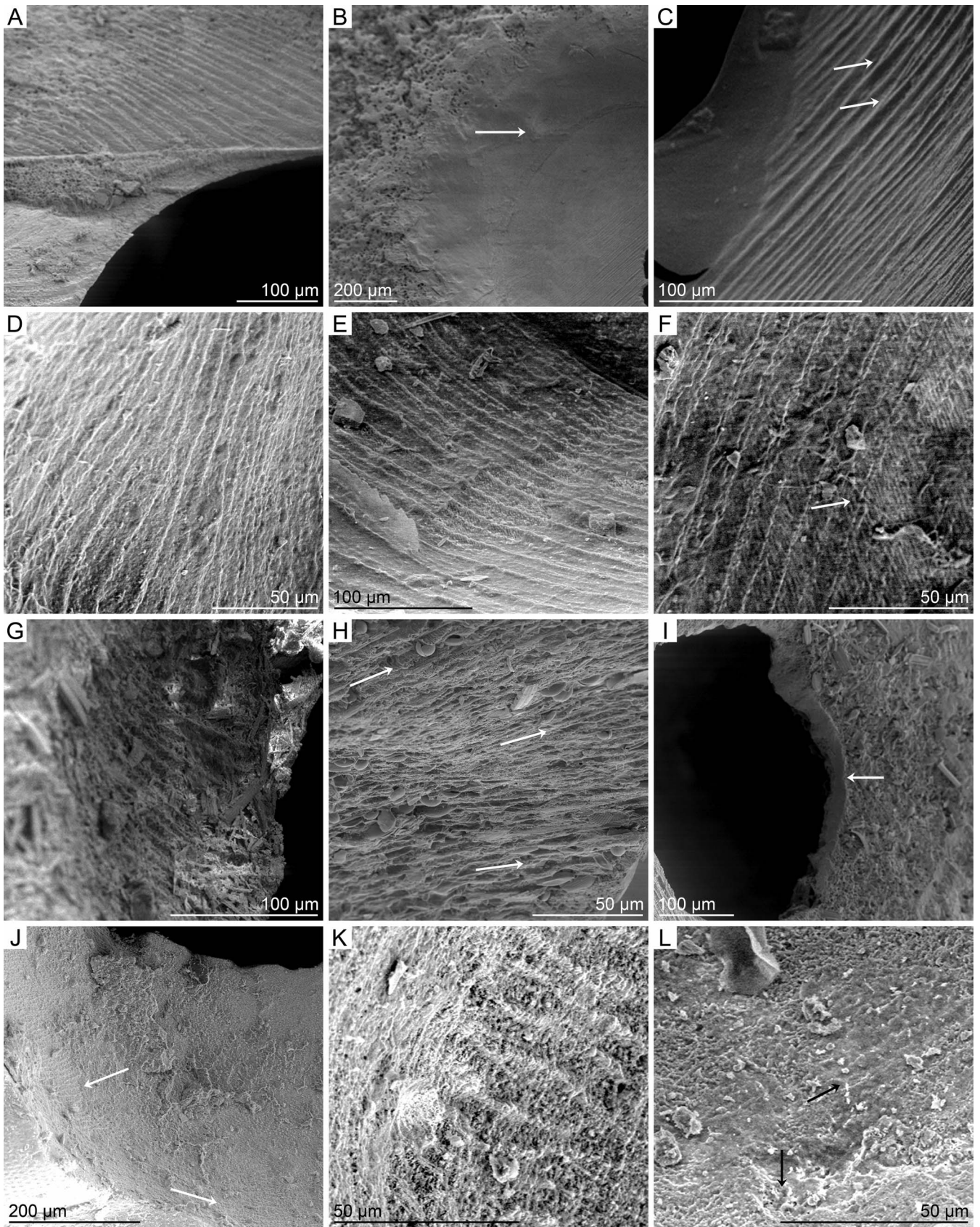
A number of randomly located drill holes examined under high-resolution FE-SEM or ESEM displayed physical scratch marks consisting of parallel to subparallel, straight to slightly curvilinear, distinctly corrugated lines. These *Radulichmus*-like lines are oriented in laterally sweeping patterns, ranging from subparallel to perpendicular to the drill-hole outline (Fig. 1). This corrugated pattern consists of indentations (or troughs) separated by raised ridges, which are interpreted as radular teeth marks (radular cusp width) and areas between the radular teeth (or inter-cusp spacing), respectively. As a proxy of radular cusp width, quantifications of microtrace spacing consisted of measuring from ridge to ridge. These measurements were evaluated for individual shells and also pooled

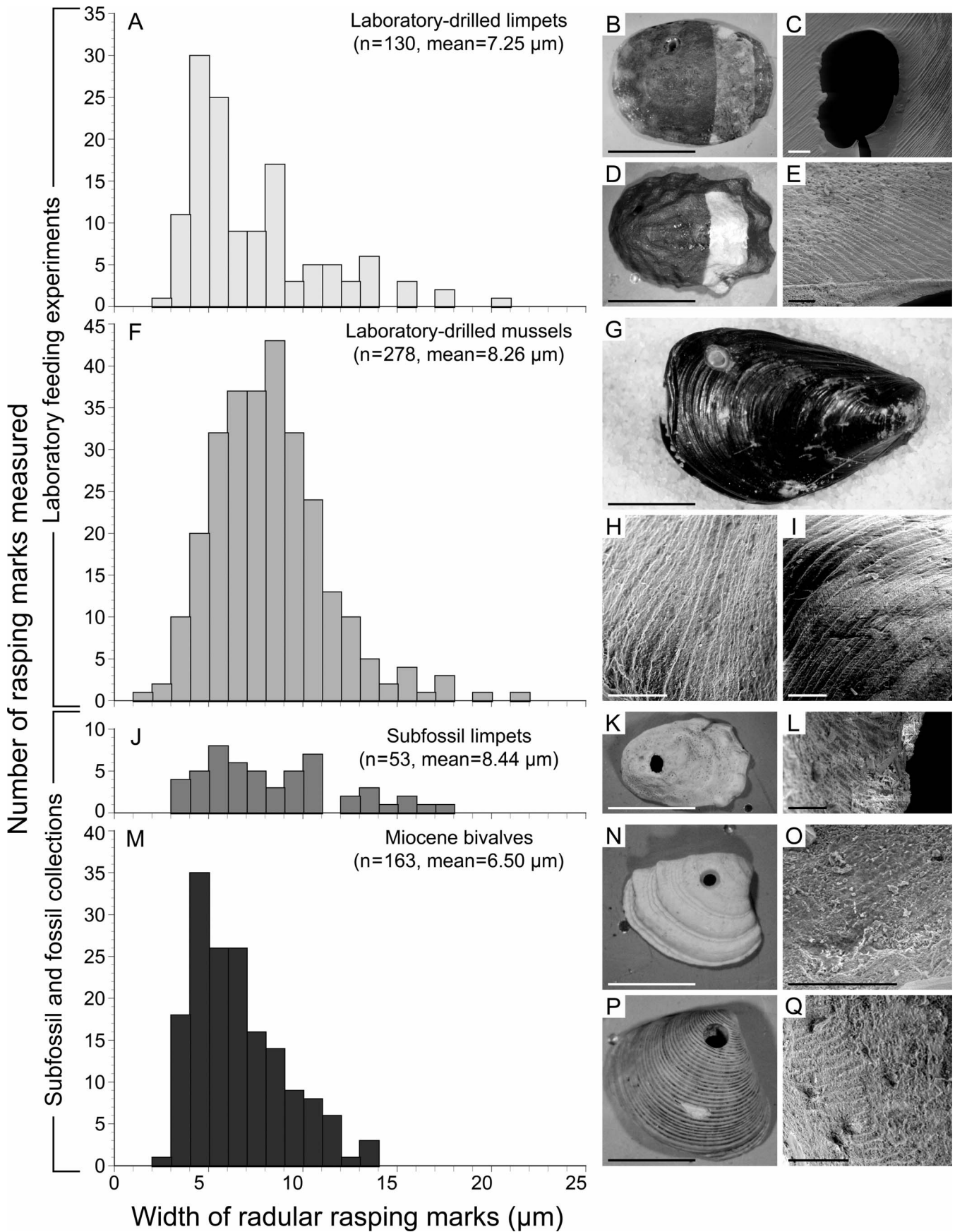
by group (as defined in Table 1; Fig. 2). The spacing of adjacent microtraces, pooled for all measured individuals, ranges from 1.84 to 21.67 μm with a mean spacing of 7.60 μm , and standard deviation of 3.13 μm ($n = 624$; pooled data histogram Fig. 3A). Spacings of the interpreted predatory microtraces, pooled by grouping and type (multiple-pass and single-pass radular microtraces), were additionally compared to crystalline shell microfabrics (Figs. 3B–D) and to radular tooth widths from the literature (Figs. 3E–F, 4A–C).

Drill Holes in Laboratory Setting on Living Organisms

Laboratory-Observed Limpets.—The two limpets (*L. digitalis* and *T. scutum*) that were drilled in the laboratory setting had *N. ostrina* predators of similar size: 21.1 mm and 24.1 mm long, by 14.6 mm and 15.7 mm wide. *Lottia digitalis* displayed a complete drill hole, with a maximum inner diameter of $\sim 770 \mu\text{m}$ (Fig. 1A), while *T. scutum* showed a non-functional (incomplete) hole, with a maximum inner diameter of $\sim 260 \mu\text{m}$ (Figs. 1B–C). Both specimens displayed quantifiable microrasping marks. The mean distance between adjacent microtraces of *L. digitalis*

FIGURE 1—Representative micro-rasping marks. A–C) FE-SEM micrographs of drill holes from limpets killed by the muricid gastropod *Nucella ostrina* in the laboratory. A) *Lottia digitalis* drill hole with perpendicular to subparallel, sweeping microtraces on margin (specimen VT-P-001). B) *Tectura scutum* outer margin of non-functional or incomplete drill hole; arrow = chemical dissolution signature (VT-P-002). C) Inner surface of *T. scutum* non-functional drill hole showing rasping microtraces perpendicular to drill-hole margin; arrows = superimposition of radular passes. D–F) ESEM micrographs of drill holes from mussel specimens killed by *Nucella lamellosa* in the laboratory. D) *Mytilus trossulus* (VT-MT-68, killed by VT-NL-34); outer drill-hole margin with parallel to slightly subparallel micro-rasping marks oriented subparallel to drill hole. E–F) *M. trossulus* (VT-MT-52, killed by VT-NL-16) showing (E) outer drill-hole margin with parallel micro-rasping marks oriented parallel to drill hole and (F) inner drill-hole margin with crystalline microstructures (arrow) oriented obliquely to the parallel micro-rasping marks; note variable spacing of rasp marks (F) compared to microtraces (E). G–I) FE-SEM micrographs of predatory drill holes from field-collected *L. digitalis* specimens. G) Parallel micro-rasping marks in *L. digitalis* (VT-2-3 C-3), oriented perpendicular to drill-hole margin. H–I) Inner drill-hole margin of *L. digitalis* (VT-1-4 B-3) showing a sweeping, fan-like pattern of micro-rasping marks (H) (arrows = outer fan edge) and possible chemical dissolution signature on inner drill-hole margin (arrow, I). J–L) ESEM micrographs of drill holes on Miocene bivalves. J) *Astarte radiata* (VT-B5-3-1) outer drill-hole margin with parallel micro-rasping marks oriented nearly perpendicular to margin (left arrow) and parallel to drill-hole margin (lower right). K) *A. radiata* (VT-B5-3-4) with perpendicularly oriented micro-rasping marks on outer drill-hole margin. L) *Clausinella basteroti* (VT-S14-11); outer drill-hole margin with possible eroded micro-rasping marks (upper arrow) and minor perforations likely associated with bioerosion (lower arrow).





was more than two times greater (11.18 μm ; $n = 42$) than that assessed for *T. scutum* (5.38 μm ; $n = 88$), a difference that is statistically significant (Mann Whitney U test, $p < 0.001$). The pooled, laboratory observed limpet microtraces ranged in size from 2.94 to 20.04 μm , with a mean spacing of 7.25 μm (Table 1, Fig. 2A). In addition to physical rasping microtraces, chemical dissolution signatures can be recognized toward the outer margin of the incomplete drill hole found on the *T. scutum* shell (Fig. 1B). In contrast, physical microrasping marks occupy the inner, depressed region of the incomplete drill hole (Fig. 1C).

Laboratory-Observed Mussels.—The six individuals selected had been drilled by one of two *N. lamellosa* predators (specimen ID# VT-NL-34 drilled two shells and VT-NL-16 drilled four shells). These specific predators were significantly larger than the *N. ostrina* specimens used in the limpet-feeding experiment, with lengths of 33.5 mm and 36.1 mm and widths of 20.8 mm and 21.1 mm for VT-NL-34 and VT-NL-16, respectively. The drill holes exhibited maximum inner diameters ranging from ~ 900 to ~ 1500 μm , and quantifiable micro-rasping marks were present on all six specimens. The mean distance between adjacent microtraces (Table 1) of *M. trossulus* pooled by predator differs significantly between the two predators (Mann Whitney U test, $p = 0.026$), with micro-rasping marks produced by the smaller snail (VT-NL-34) averaging 7.64 μm ($n = 89$) and those produced by the larger snail (VT-NL-16) averaging 8.55 μm ($n = 189$). In total, the pooled laboratory-observed mussel microtraces ranged in size from 1.84 to 21.67 μm , with a mean spacing of 8.26 μm (Table 1, Fig. 2F). Two specimens illustrated possible chemical dissolution signatures in addition to physical predatory microtraces. In contrast to the dissolution signatures observed on the laboratory-drilled *T. scutum* specimen, the putative chemical signatures were located towards the inner drill-hole margin, with radular microtraces occupying the outer drill-hole margin. Additionally, the chemical dissolution features noted here appear comparatively rough and give the impression of erosional or bioerosional surfaces commonly observed in the subfossil and fossil specimens.

Published Nucella Radula Micrographs.—Two published scanning electron micrographs (Rolán et al., 2004, fig. 2E–F; see Fig. 3F) of the radula of the dogwhelk *N. lapillus* were analyzed for comparative purposes. Because these radulae came from drilling predators congeneric to those used in the two laboratory feeding experiments, they should display similar radular morphologies. Moreover, the two radula illustrated in Rolán et al. (2004) came from muricids of similar sizes to those used in the feeding experiments (lengths of 26.2 mm and 25.9 mm, respectively). Individual cusp widths ranged from 11.53 to 21.36 μm , with a mean cusp width of 15.26 μm ($n = 45$; Table 1, Fig. 3E).

Drill Holes in Subfossil and Fossil Organisms

Subfossil Limpets.—Ten drilled subfossil shells of *L. digitalis* were examined for microstructural features under FE-SEM. The majority of the individuals recovered showed signs of substantial taphonomic degradation, including fragmentation, loss of color, corrosion (deterioration and abrasion), bioerosion (microperforations not caused by predation or parasitism), and encrustation. Nevertheless, four of the ten shells preserve distinct micro-rasping marks around the drill-hole margins (Figs. 1G–I), one of which contains radular microtraces oriented in a sweeping, fan-like pattern (Fig. 1H). These four drill holes exhibited maximum inner diameters of ~ 360 to ~ 670 μm . The distance between micro-rasping

marks illustrated a mean of 8.44 μm and ranged from 3.58 to 17.31 μm ($n = 53$; Table 1, Fig. 2J). One specimen contained a tenuous chemical dissolution signature in addition to physical rasping microtraces (Fig. 1I). Much like those of the laboratory-drilled mussels, the possible chemical dissolution signature appeared rutted and was located towards the inner drill-hole margin, with radular microtraces and indications of bioerosion occupying the outer drill-hole margin.

Miocene Bivalves.—The majority of the twelve Miocene bivalves examined displayed signs of substantial taphonomic degradation. A total of three shells illustrated easily identifiable micro-rasping marks around the drill-hole margins, including two *A. radiata* shells (Burdigalian) and the *C. basteroti* specimen (Langhian) (Figs. 1J–L). The maximum inner diameters of these three drill holes ranged from ~ 650 to ~ 1070 μm , and the micro-rasping marks ranged from 2.51 to 13.58 μm with a mean of 6.50 μm ($n = 163$; Table 1, Fig. 2M).

The observed subfossil and fossil predatory microtraces are located in direct proximity to the drill-hole margins and bear close resemblance to microtraces observed around the laboratory-observed drill holes for both limpets and mussels. The spacing of individual micro-rasping marks is comparable (overlapping) to those observed in the laboratory data. Distinct chemical dissolution signatures observed for the incomplete drill hole obtained in the laboratory could not be confidently identified for any of the field-collected subfossil and fossil specimens.

Multiple-Pass and Single-Pass Micro-Rasping Marks

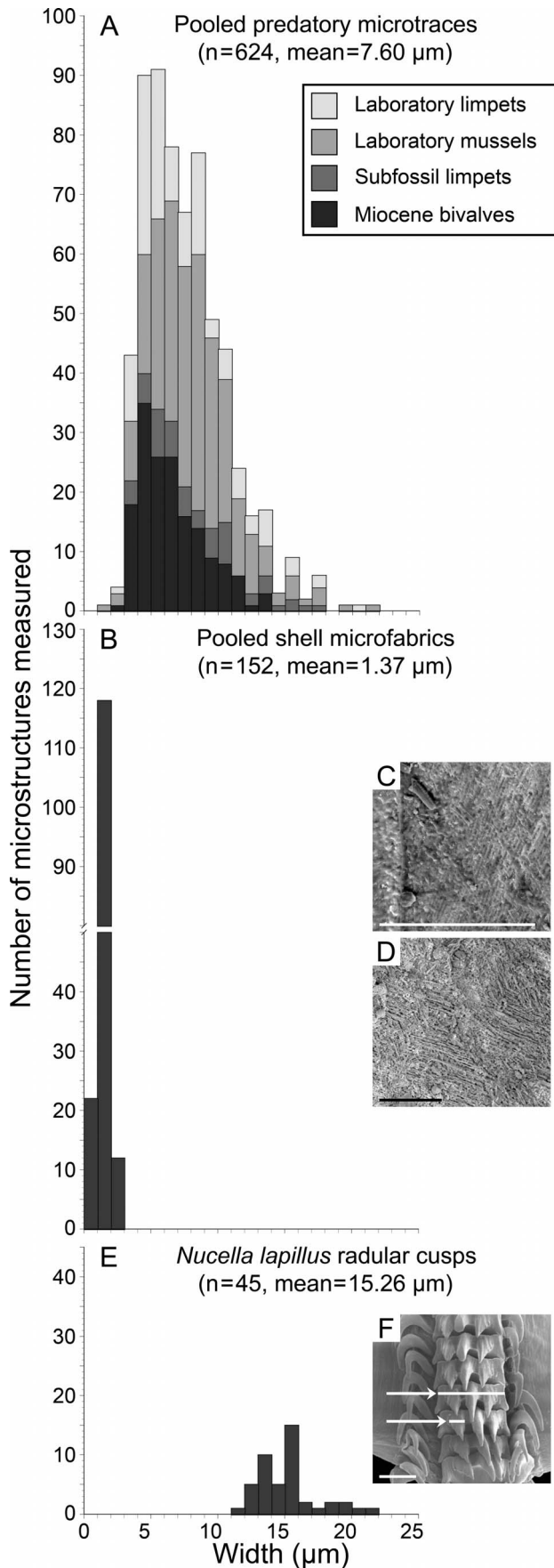
In order to further categorize the rasping microtraces, the measured images from all four groupings were selected, pooled, and comparatively evaluated in two categories: (1) clearly overlain micro-rasping marks—i.e., multiple, superimposed radular-pass microtraces (Figs. 4D–G), which ranged in size from 1.84 to 11.21 μm (mean = 5.75 μm , $n = 149$); and (2) micro-rasping marks that show no evidence of superimposition—i.e., single radular-pass microtraces (Figs. 4H–K), which ranged in size from 4.18 to 21.67 μm (mean = 10.31 μm , $n = 108$) (Table 1, Figs. 4A–B). These two distributions are significantly different from each other, as well as from the literature-assessed radular tooth widths (Mann Whitney U test, in all three cases $p < 0.001$).

Shell Crystalline Microarchitecture

Two of the six laboratory-drilled mussels analyzed illustrated quantifiable crystalline microfabrics oriented subparallel to the radular microtraces (Figs. 1F, 3C), which ranged in size from 0.53 to 2.57 μm (mean = 1.48 μm , $n = 102$). The laboratory-drilled *L. digitalis* limpet specimen showed hints of crystalline microfabrics oriented subparallel to the radular microtraces (Fig. 4H), which are similar, although less continuous and pronounced, to crystalline microfabrics observed in the laboratory-drilled mussels. These structures were not quantified, as their interpretation remains tenuous. In addition to the quantified mussel microfabrics, one of the Miocene bivalve specimens, *A. radiata* from the Winterswijk-Miste area, showed a crossed-lamellar microfabric on a fracture surface (Fig. 3D). These lamellae illustrated a similar, but narrower, range to those ascertained from the two mussel specimens, extending from 0.66 to 1.75 μm , with a mean of 1.17 μm , ($n = 50$). The pooled crystalline microfabrics ranged from 0.53 to 2.57 μm (mean = 1.37 μm , $n = 152$; Table 1, Fig. 3B).

←

FIGURE 2—Predatory microtrace size-frequency distributions and images of corresponding shells. Spacing between micro-rasping marks measured to the nearest 0.01 μm . A, F, J, M) Microtrace spacing distribution of laboratory-drilled shells; for histogram shading, see Figure 3. B–E) Shells of *Tectura scutum* (B–C, specimen VT-P-002) and *Lottia digitalis* (D–E, VT-P-001) with corresponding electron micrographs illustrating measured predatory microtraces (lighter strip on shells in B and D represents area covered by conductive copper tape where specimen was not sputter coated). G–I) *Mytilus trossulus* showing representative specimen (G) and electron micrographs of predatory microtraces drilled by *Nucella lamellosa* (H–I, VT-NL-16 and VT-NL-34, respectively). K–L) Representative subfossil *L. digitalis* and electron micrograph of predatory microtraces. N–Q) Miocene bivalves *Clausinella basteroti* (N–O, VT-S14-11) and *Astarte radiata* (P–Q, VT-B5-3-1) with corresponding electron micrographs illustrating predatory microtraces. Photographic scale bars = 0.5 cm; SEM scale bars = 50 μm .



DISCUSSION

The predatory drilling process involves intermittent use of the accessory boring organ, located in the foot of muricids, and the radula. The accessory boring organ reduces the structural integrity of the prey's calcium carbonate shell and proteinaceous matrix via secretion of ion chelating agents (acids and enzymes), and the radula physically rasps the weakened shell material away (Carriker, 1981). We infer that the microtraces observed in high-resolution FE-SEM and ESEM micrographs represent this rasping motion and consequent removal of shell material, as has been suggested in earlier studies on modern prey shells such as oysters and mussels (Carriker, 1969, 1978; Carriker and Van Zandt, 1972). Two hypotheses can be proposed to explain the microtrace spacing variation among these groups: (1) predator taxonomy and size may induce variations in radular cusp size or radular intercusp spacing, thus affecting the spacing of the micro-rasping marks observed on the prey shells; and (2) observed microtrace spacing may result from overprinting of multiple radular passes.

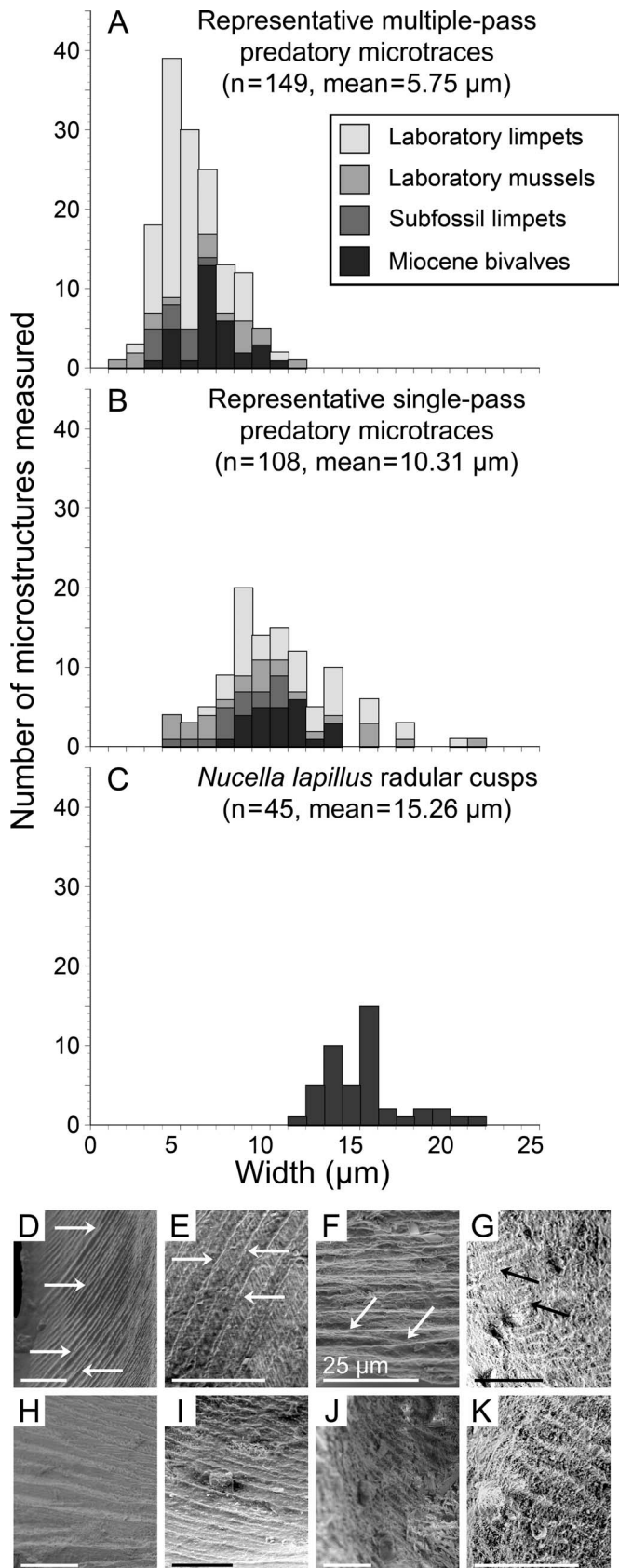
Primary Hypotheses to Explain Predatory Microtrace Variations

Predator Taxonomy and Size-Age Class.—Differences in radular size and cusp spacing may be related to intergeneric distinctions in radular morphology as well as variations in predator size or age class. The two muricid predators (*N. ostrina*) responsible for drilling in the limpet-feeding experiment differed by only a few millimeters in size (3.0 mm in length); the predator that drilled *L. digitalis* was slightly smaller than the one that drilled *T. scutum*. The primary assumption was that larger predators would produce more widely spaced micro-rasping marks. Accordingly, due to the roughly similar sizes of these two predator individuals, the spacings of the microtraces generated were expected, *a priori*, to differ proportionally with predator size, but not dramatically. The difference in microtrace spacing means between these two predators, 5.80 μm (11.18 μm mean for *L. digitalis*, 5.38 μm mean for *T. scutum*; Mann Whitney U test, $p < 0.001$), however, was much larger than anticipated. In fact, the two species of limpets showed an appreciably wide variation of microtrace spacing, nearly reaching the range endpoints of all examined shells, including both subfossil and fossil shells. Moreover, the larger dogwinkle predator that drilled *T. scutum* produced more tightly spaced micro-rasping marks.

In the mussel-feeding experiments, the two *N. lamellosa* predators again varied in size by only a few millimeters (a difference of 2.6 mm in length). Based on size differences in the predators, the distances between radular microtraces on the mussel prey shells were anticipated to differ respectively—if much at all. Although the microtrace spacing variation between predators observed in the mussels was much less than that of the limpets, the difference was again statistically significant. The predators used in the mussel-feeding experiments were nearly 10 mm larger than those used in the limpet-feeding experiments, so a larger relative difference between pooled means would be expected. Because the microtrace spacing means for laboratory-drilled limpets illustrated a difference of nearly 6 μm between prey drilled by the two different predators, a difference in mean rasp-mark spacing between pooled laboratory experiments of only 1.01 μm was unexpected (8.26 μm mean for pooled mussels, 7.25 μm mean for pooled limpets; Mann Whitney U test, $p <$

←

FIGURE 3—Predatory microtrace, shell microstructure, and radular cusp data. A) Size-frequency distribution of spacing between rasping marks for all analyzed drill holes. B) Size-frequency distribution of crystalline mussel-shell microstructures. C) Electron micrograph of mussel-shell fibrous prismatic microfabric. D) Electron micrograph of Miocene *Astarte radiata* shell crossed-lamellar microfabric. E) Radular cusp widths measured from Rolán et al. (2004). F) Radular cusps of *N. lapillus*, upper arrow indicates rachidian tooth containing three radular cusps; line = tooth width. Lower arrow indicates single radular cusp; line = cusp width (modified from fig. 2E of Rolán et al., 2004). Scale bars in C, D, and F = 50 μm .



0.001). Unfortunately, even with statistically significant results, no quantitatively prognostic statements can be made relating predator size to radular microtrace-spacing distances due to the irregular and unpredictable magnitudes by which the spacings differ from case to case.

Despite substantial taphonomic alterations, multiple subfossil and fossil specimens preserve a distinct predatory microstructural signature associated with the drilling process or predatory microtraces. The notable differences in rasp-mark spacing are difficult to evaluate given that the size and specific taxonomic identity of predators that drilled the field-collected shells are unknown. Indeed, in regard to the subfossil-collected assemblage, not only do False Bay muricids vary notably in size as observed in the field, but field studies also (e.g., Palmer, 1988) indicate that there are at least two more *Nucella* species that may drill limpets in the study area, *N. lima* (Gmelin) and *N. canaliculata* (Duclos). Certainly, multiple species of drilling gastropods (from varying size or age classes) were present throughout the sampled European Miocene deposits (Hoffmeister and Kowalewski, 2001; Kowalewski et al., 2002). The distances between rasping microtraces around the drill holes of subfossil limpet shells (ranging from 3.58 to 17.31 μm) and Miocene bivalve shells (2.51–13.58 μm) overlap with the range of values reported above for laboratory-observed drill holes (Table 1, Figs. 2A, F, J, M).

A pertinent test for effects of predator size on radular microtrace spacing undoubtedly exists, although we could not evaluate this issue more rigorously in the current experimental design, as the animals used in the limpet experiment were released unharmed after the study to protect local snail populations, and the specimens in the mussel-feeding experiment were too highly degraded after four years in alcohol to remove the radula intact. It is noteworthy that the minimum radular tooth widths (11.53 μm) measured from similar-sized congeneric dogwhelks (Rolán et al., 2004) overlap with the predatory microtrace spacings measured in all laboratory specimens. Nearly 15% (60 of 408) of the measured micro-rasping marks have spacings ≥ 11.53 μm , although comparisons of the overall measurement distributions are significantly different (Mann Whitney U test, $p < 0.001$). Because the drilling muricids examined by Rolán et al. (2004) are closely related, and morphologically similar, to those used in the feeding experiments here, they should display relatively similar radular morphologies and drilling methodologies versus, for example, a comparison with the radular morphologies and drilling methodologies of naticid or cassid gastropods. The difference between maximum values for radular cusp width (21.36 μm) and microtrace spacings among all laboratory-observed drill holes (21.67 μm) is only 0.31 μm , which is certainly reasonable given that radular size and morphology may vary considerably across predator size and age classes. The maximum value for the pooled subfossil and fossil microtrace spacings (17.31 μm) is 4.05 μm smaller than the upper limit of the radular cusp width range, and $\sim 9\%$ (20 of 216) of the measured subfossil-fossil microtrace spacings are ≥ 11.53 μm . Again, the distributions remain statistically different (Mann Whitney U test, $p < 0.001$). The proximity of rasp-mark spacings between the subfossil-fossil drill holes and the radular cusp widths assessed from Rolán et al. (2004), however, is obviously less meaningful than that calculated for the laboratory-observed micro-rasping marks, but this is to be expected with the lack of information on predator taxonomy, size, and age class.

←

FIGURE 4—Size differentiation of multiple-pass (overlain) and single-pass predatory microtraces (A–B) versus distribution of radular cusp widths in *N. lapillus* (C), as measured from Rolán et al. (2004). D–G) Representative multiple-pass predatory microtraces from: D) a laboratory-observed limpet (specimen VT-P-002), E) a laboratory-observed mussel (VT-MT-52, left margin), F) a subfossil limpet (VT-1-4 B-3), and G) Miocene *Astarte radiata* (VT-B5-3-1). Arrows indicate points of cross-cutting radular marks. H–K) Representative single-pass predatory microtraces from: H) a laboratory-observed limpet (VT-P-001), I) a laboratory-observed mussel (VT-MT-52, bottom margin), J) a subfossil limpet (VT-2-3 C-3), and K) *A. radiata* (specimen VT-B5-3-4). All scale bars = 50 μm unless otherwise labeled.

Although the radulae used for comparative analyses were preserved in alcohol (Rolán et al., 2004), which may cause radular shrinkage, it was still possible to assess the basal cusp widths. As the drill-hole microtrace widths should correlate closely to depth of radular cusp penetration, using the basal cusp widths approximates a maximum value for predatory microtrace-spacing. That is, radular passes with less pressure should produce more narrowly spaced rasping microtraces, as only the tip of the radular cusps would penetrate the shell material; conversely, deeply penetrating radular passes should be nearer to the basal width of the radular cusps. Varying widths of the predatory microtraces should be expected, however, as the scenarios described above simply represent end members of the range.

Superimposition of Radular Passes.—The differences in microtrace spacing may be induced by the superimposition of multiple radular passes (visible in Figs. 1C, 4D–G), which is perhaps more likely than differences resulting from predator size variation. In this scenario, the differences in microtrace spacing represent a composite of sequential overlying raspings on the drilled region of the prey shell. It has been proposed that mechanical radular rasping plays a relatively minor role in the drilling process, functioning to remove chelated prey shell material (Carriker, 1981). A study on drilling predation by modern *N. lapillus* on *Mytilus edulis* (Linnaeus) prey, however, proposes a more extensive role for the radula, in which the first quarter of the drilling process consists of “frequent and intense mechanical scraping” by the radula, broken by periods of inactivity, inferred as shell chelation (Rovero et al., 1999, p. 1083). The case for superimposition of radular rasping, or multiple radular passes, is supported by the rachidian cusp widths measured from published *N. lapillus* SEM micrographs (Rolán et al., 2004), where the mean cusp width (15.26 μm) was approximately double the mean of the pooled rasping microtraces (7.60 μm) and, more specifically, the feeding experiment micro-rasping marks (7.94 μm). Detailed information about radular teeth spacing from drill-hole microtrace spacing could be disputable, however, because it may not be feasible to distinguish an earlier radular pass from any later passes. It may be worthwhile to examine variation among the inner drill-hole-region microtrace spacing, particularly in incomplete drill holes, versus that of the outer drill-hole margin. Presumably, the outer margin of drill holes should not receive as many radular passes as the central region of the bored area because less prey shell material is removed along the outer margin. Thus, the lower number of overlapping radular rasp marks along the outer margin may have more diagnostic value in relation to radular cusp width of the predator. Ultimately, the best-case scenario would be the identification of pristine, single radular passes. In more heavily rasped regions of the drill hole, it is challenging to discern (1) the number of overlapping radular passes and (2) the amount or spacing of overlap. Therefore, extracting any meaningful data on radular cusp width in such areas is unlikely, and such data would also be contentious.

It is most likely that, as the drilling process proceeds, the fluids released by the accessory boring organ reduce or obscure earlier micro-rasping marks and create a smoothed dissolution halo around the outer rim of the drill-hole cavity. During the final stages of penetration, rasping may overprint and obscure evidence for dissolution around the inner opening. While no definitive chemical dissolution features were observed in any subfossil or fossil shells, one unambiguous dissolution feature was observed in the incomplete drill hole produced in the limpet laboratory experiment. Chemical dissolution signatures in previous laboratory experiments were observed when the drilling process was interrupted (Carriker, 1969; Carriker and Van Zandt, 1972), and distinct chemical dissolution halos were observed in complete drill holes (interpreted as cassid gastropod drillings) found in echinoid tests (Nebelsick and Kowalewski, 1999). Although not always present or discernible, the predatory microstructural gradient documented in the laboratory-observed incomplete drill hole—with physical micro-rasping marks located proximally and a chemical dissolution halo more distally—represents a distinct signature of chemically aided radular drilling. The equivocal chemical dissolution

signatures toward the inner drill-hole margins from two of the laboratory-observed mussels and one of the subfossil limpets may represent variations in shell structure toward the inner surface of the shell or a period of chemically aided dissolution just prior to the final puncturing of the prey shell.

If an accurate depth-profile of radular marks could be attained, presumably the most recent pass would generate the deepest and most pristine microtraces, while microtraces generated in earlier passes would be less pronounced or more eroded. Although obtaining precise three-dimensional measurements is difficult, a distinction can be made between more pristine, single radular passes and overlying, multiple passes by searching for signs of crosscutting within the predatory microtraces, and this characteristic may provide a means to further resolve microtrace spacing. To test this idea, representative multiple-pass and single-pass micro-rasping marks from all four primary groupings of shells were comparatively evaluated. The range of multiple-pass predatory microtrace widths does not intersect the distribution of radular tooth widths (Figs. 4A, C), while the distribution of single-pass predatory microtrace widths is closer to, and overlaps the distribution of radular tooth widths, with slightly more than 35% (38 of 108) overlap (Figs. 4B, C).

Microtraces and Shell Crystalline Microarchitecture.—An alternative interpretation of the predatory microtraces is that their morphology reflects the crystal fabric of the shells. In the laboratory-drilled mussels, two of the six mussels illustrated crystalline fabrics that are unambiguously oriented subparallel to the radular rasping marks (Figs. 1E, 3C). Additionally, one of the Miocene bivalves illustrated typical crossed-lamellar growth fabrics (Fig. 3D) (for SEM of shell microarchitectures, see Carter, 1990a, 1990b; Herbert, 2005). When the pooled crystalline microfabric measurements, ranging from 0.53 to 2.57 μm wide (mean = 1.37 μm , $n = 152$, Table 1), are compared to the overall range of predatory microtrace sizes, the larger end of the crystalline microfabric range only slightly overlaps the smallest radular microtraces (8.6% overlap; 13 of 152 microfabric elements are larger than the smallest rasp mark (1.84 μm). This difference is statistically significant (Mann Whitney U test, $p < 0.001$). Conversely, the smallest observed predatory microtraces overlap the crystalline microfabric range by a mere 0.48%. Only three of 624 predatory microtraces were $\leq 2.57 \mu\text{m}$, the maximum size of the crystalline elements. In the mussels, the crystalline microstructures are organized predominantly into fibrous prismatic bundles, which group together into higher-order structural growth packages. At first inspection, the radular marks reported here may be mistakenly identified as either individual bundles or larger structural packages of bundles. The size and arrangement of these bundles and higher-order packages, however, is consistent from individual to individual, due to the regularity of shell growth patterns within species. On the other hand, the rasp marks vary in spacing, direction relative to drill-hole margin, and orientation relative to the crystalline bundles, all of which distinguish them from features of the shell microstructure. In addition, no combination of the shell-growth microfabrics has been observed to produce the larger, corrugated pattern of ridges and troughs formed by the rasp marks, a pattern which varies in direction from shell to shell. Many of the rasping marks not only change direction within single drill holes, but also cut across one another, which would not be expected if they were merely expressions of the underlying growth layers. Perhaps most convincing is the incomplete drill hole observed in one of the laboratory-drilled limpets showing distal chemical-dissolution features, with superimposed micro-rasping marks in the central drill-hole depression. Because chemical dissolution serves to reduce or smooth the topographical expression of the crystalline shell microarchitecture, the superposition of parallel rasping microtraces on top of this smoothed area provides further evidence to separate the rasping marks from any shell-growth microfabrics. Lastly, radular rasp marks have a similar morphology, regardless of species of prey, while shell structure varies from prismatic, crossed-lamellar, and fibrillar in limpets (Lindberg, 1988) to irregular, complex crossed-lamellar and fibrous prismatic bundles in mussels (Carter and Lutz, 1990), to crossed-lamellar in Miocene

bivalves (Carter and Lutz, 1990). This consistency of predatory-microtrace morphology despite differences in the prey-shell crystalline microfabrics suggests that shell microarchitecture plays a negligible role in predatory interpretations. Furthermore, due to differences in scale, orientation, and arrangement between the predatory microtraces and the prey-shell crystalline microarchitectures, we suggest that the microtraces reported here are distinctly not expressions of underlying shell microarchitectures.

CONCLUSIONS

The numerical evaluation and diagnostic value of predatory microtrace spacing deserves attention and provides intriguing avenues for future research. In particular, experimental studies that would jointly consider SEM micrographs of rasping microtraces and radular morphology and cusp width of their producers could help to evaluate the anatomical fidelity of these microtraces. Moreover, as these radular corrugations seem randomly oriented, future examinations may focus on more stringently assessing rasp-mark orientation with regard to location of the drill hole on the prey shell and variation of prey-shell crystalline microarchitectures.

The presence of such predatory microtraces, especially in true fossil specimens, may provide a viable tool for identifying taphonomically degraded or irregularly shaped drill holes that would otherwise be dismissed by researchers. Likewise, dissolution signatures, which can be preserved around drill-hole margins in well-preserved fossils, may help us to evaluate whether the drilling process was chemically aided—an important criterion for identifying the presence of accessory boring organs or similar structures in ancient predators. Although chemical dissolution signatures have been observed in numerous modern drill holes, the quantification of predatory microtrace spacing may have more diagnostic value in evaluating predator-prey interactions. Finally, distinct microtraces of radular rasping that can be readily identified and numerically evaluated using SEM techniques offer promise for augmenting our ability to identify drill holes from fossil specimens, especially when fossils are degraded or when drilling organisms are difficult to infer independently.

ACKNOWLEDGMENTS

The experimental portions of this study were conducted at the Friday Harbor Laboratories during a Predator-Prey Interactions summer course. We would like to thank the FHL faculty and staff for providing funding, facilities, and logistic and intellectual support. All EM analyses were conducted at the Virginia Tech Institute for Critical Technology and Applied Science Nanoscale Characterization and Fabrication Laboratory (ICTAS-NCFL). The final stages of the study were partly supported by National Science Foundation grant (OCE-0602375). We thank J.W. Huntley (University of Kentucky) for his generous help during the FHL summer course and for insights on the manuscript; S.R.F. McCartney and J. McIntosh (ICTAS-NCFL) for FE-SEM and ESEM technical assistance; and T.A. Dexter, P.J. Voice, A.F. Wallace, and S. Xiao (Virginia Tech) for constructive comments on earlier drafts of this report. We also thank G.S. Herbert (University of South Florida) for valuable discussions, as well as K. Parsons-Hubbard (Oberlin College), E.M. Harper (Cambridge University), two anonymous reviewers, and an anonymous associate editor for constructive reviews, suggestions, and comments that greatly improved the quality of this manuscript.

REFERENCES

- CARRIKER, M.R., 1969, Excavation of boreholes by the gastropod, *Urosalpinx*: An analysis by light and scanning electron microscopy: *American Zoologist*, v. 9, p. 917–933.
- CARRIKER, M.R., 1978, Ultrastructural analysis of dissolution of shell of the bivalve *Mytilus edulis* by the accessory boring organ of the gastropod *Urosalpinx cinerea*: *Marine Biology*, v. 48, p. 105–134.
- CARRIKER, M.R., 1981, Shell penetration and feeding by naticacean and muricacean predatory gastropods: A synthesis: *Malacologia*, v. 20, p. 403–422.
- CARRIKER, M.R., and VAN ZANDT, D., 1972, Predatory behavior of a shell-boring muricid gastropod, in Winn, H.E., and Olla, B.L., eds., *Behavior of Marine Animals: Current Perspectives in Research*: Plenum, New York, p. 157–244.
- CARTER, J.G., ed., 1990a, *Skeletal Biomineralization: Patterns, Processes and Evolutionary Trends, Volume 1*: Van Nostrand Reinhold, New York, 597 p.
- CARTER, J.G., ed., 1990b, *Skeletal Biomineralization: Patterns, Processes and Evolutionary Trends, Atlas and Index, Volume 2*: Van Nostrand Reinhold, New York, 200 p.
- CARTER, J.G., and LUTZ, R.A., 1990, Bivalvia (Mollusca), in Carter, J.G., ed., *Skeletal Biomineralization: Patterns, Processes and Evolutionary Trends, Atlas and Index*: Van Nostrand Reinhold, New York, p. 5–121.
- DIETL, G.P., and KELLEY, P.H., 2006, Can naticid gastropod predators be discriminated by the holes they drill?: *Ichnos*, v. 13, p. 103–108.
- GREY, M., BOULDING, E.G., and BROOKFIELD, M.E., 2005, Shape differences among boreholes drilled by three species of naticid gastropods: *Journal of Molluscan Studies*, v. 71, p. 253–256.
- HAMMER, O., HARPER, D.A.T., and RYAN, P.D., 2001, PAST—Paleontological Statistics Software Package for Education and Data Analysis: *Palaentologica Electronica*, v. 4, no. 1, art. 4: 178 KB; http://palaeo-electronica.org/2001_1/past/issue1_01.htm. Checked July 10, 2008 (software available, <http://folk.uio.no/ohammer/past/download.html>).
- HERBERT, G.S., 2005, Systematic revision of the genus *Eupleura* H. and A. Adams, 1853 (Gastropoda: Muricidae) in the Neogene to Recent of Tropical America: *The Veliger*, v. 47, p. 294–331.
- HOFFMEISTER, A.P., and KOWALEWSKI, M., 2001, Spatial and environmental variation in the fossil record of drilling predation: A case study from the Miocene of Central Europe: *PALAIOS*, v. 16, p. 566–579.
- HOFFMEISTER, A.P., KOWALEWSKI, M., BAMBACH, R.K., and BAUMILLER, T.K., 2003, Intense drilling in the Carboniferous brachiopod *Cardiarina cordata* Cooper, 1956: *Lethaia*, v. 36, p. 107–117.
- HUNTLEY, J.W., and KOWALEWSKI, M., 2007, Strong coupling of predation intensity and diversity in the Phanerozoic fossil record: *Proceedings of the National Academy of Sciences, USA*, v. 104, p. 15006–15010.
- KAPLAN, P., and BAUMILLER, T.K., 2001, A misuse of Occam's Razor that trims more than just the fat: *PALAIOS*, v. 16, p. 525–527.
- KELLEY, P.H., 1988, Predation by Miocene gastropods of the Chesapeake Group: stereotyped and predictable: *PALAIOS*, v. 3, p. 436–448.
- KELLEY, P.H., and HANSEN, T.A., 2006, Comparisons of class- and lower taxon-level patterns in naticid gastropod predation, Cretaceous to Pleistocene of the US Coastal Plain: *Palaogeography, Palaeoclimatology, Palaeoecology*, v. 236, p. 302–320.
- KITCHELL, J.A., BOGGS, C.H., KITCHELL, J.F., and RICE, J.A., 1981, Prey selection by naticid gastropods: Experimental tests and application to the fossil record: *Paleobiology*, v. 7, p. 533–552.
- KOWALEWSKI, M., 1993, Morphometric analysis of predatory drillholes: *Palaogeography, Palaeoclimatology, Palaeoecology*, v. 102, p. 69–88.
- KOWALEWSKI, M., 2002, The fossil record of predation: An overview of analytical methods, in Kowalewski, M., and Kelley, P.H., eds., *The Fossil Record of Predation*: Paleontological Society Special Papers, Yale Printing Service, New Haven, Connecticut, p. 3–42.
- KOWALEWSKI, M., 2004, Drill holes produced by the predatory gastropod *Nucella lamellosa* (Muricidae): Paleobiological and ecological implications: *Journal of Molluscan Studies*, v. 70, p. 359–370.
- KOWALEWSKI, M., DULAI, A., and FÜRSICH, F.T., 1998, A fossil record full of holes: The Phanerozoic history of drilling predation: *Geology*, v. 26, p. 1091–1094.
- KOWALEWSKI, M., GÜRS, K., NEBELSICK, J.H., OSCHMANN, W., PILLER, W.E., and HOFFMEISTER, A.P., 2002, Multivariate hierarchical analyses of Miocene mollusk assemblages of Europe: Paleogeographic, paleoecological, and biostratigraphic implications: *GSA Bulletin*, v. 114, p. 239–256.
- KOWALEWSKI, M., HOFFMEISTER, A.P., BAUMILLER, T.K., and BAMBACH, R.K., 2005, Secondary evolutionary escalation between brachiopods and enemies of other prey: *Science*, v. 308, p. 1774–1777.
- LEIGHTON, L.R., 2001, New example of Devonian predatory boreholes and the influence of brachiopod spines on predator success: *Palaogeography, Palaeoclimatology, Palaeoecology*, v. 165, p. 53–69.
- LEIGHTON, L.R., 2002, Inferring predation intensity in the marine fossil record: *Paleobiology*, v. 28, p. 328–342.
- LEIGHTON, L.R., 2003, Morphological response of prey to drilling predation in the Middle Devonian: *Palaogeography, Palaeoclimatology, Palaeoecology*, v. 201, p. 221–234.
- LESCINSKY, H.L., and BENNINGER, L., 1994, Pseudo-borings and predator traces: Artifacts of pressure-dissolution in fossiliferous shales: *PALAIOS*, v. 9, p. 599–604.
- LINDBERG, D.R., 1988, *The Patellogastropoda*: Malacological Review, Supplement v. 4, p. 35–63.
- NEBELSICK, J.H., and KOWALEWSKI, M., 1999, Drilling predation on recent clypeasteroid echinoids from the Red Sea: *PALAIOS*, v. 14, p. 127–144.

- PALMER, A.R., 1988, Feeding biology of *Ocenebra lurida* (Prosobranchia: Muricea): Diet, predator-prey, size relations, and attack behavior: *The Veliger*, v. 31, p. 192–203.
- ROLÁN, E., GUERRA-VARELA, J., COLSON, I., HUGHES, R.N., and ROLÁN-VAREZ, E., 2004, Morphological and genetic analysis of two sympatric morphs of the dogwhelk *Nucella lapillus* (Gastropoda: Muricidae) from Galicia (northwestern Spain): *Journal of Molluscan Studies*, v. 70, p. 179–185.
- ROVERO, F., HUGHES, R.N., and CHELAZZI, G., 1999, Automatic recording of the radular activity of dogwhelks (*Nucella lapillus*) drilling mussels (*Mytilus edulis*): *Journal of the Marine Biological Association of the United Kingdom*, v. 79, p. 1079–1083.
- SHEEHAN, P.M., and LESPERANCE, P.J., 1978, Effect of predation on the population dynamics of a Devonian brachiopod: *Journal of Paleontology*, v. 52, p. 812–817.
- URRUTIA, G.X., and NAVARRO, J.M., 2001, Patterns of shell penetration by *Chorus giganteus* juveniles (Gastropoda: Muricidae) on the mussel *Semimytilus algosus*: *Journal of Experimental Marine Biology and Ecology*, v. 258, p. 141–153.
- VERMEIJ, G.J., 1987, *Evolution and Escalation: An Ecological History of Life*: Princeton University Press, New Jersey, 527 p.
- WALKER, S.E., 2007, Traces of gastropod predation on molluscan prey in tropical reef environments, in Miller III, W., ed., *Trace Fossils: Concepts, Problems, and Prospects*: Elsevier, Amsterdam, p. 324–344.
- WILSON, M.A., and PALMER, T.J., 2001, Domiciles, not predatory borings: A simpler explanation of the holes in Ordovician shells analyzed by Kaplan and Baumiller, 2000: *PALAIOS*, v. 16, p. 524–525.

ACCEPTED JUNE 24, 2008